DOI: 10.24996/ijs.2025.66.7.25

ISSN: 0067-2904

Eye Iris Classification Using the Alex Net Model with Absolute Activation Function

Bahera H. Nayef
Department of Computer Science, College of Science, Al Nahrain University, Baghdad, Iraq

Received: 18/1/2024 Accepted: 14/8/2024 Published: 30/7/2025

Abstract:
Eye iris classification and recognition are important in pattern recognition applications. Traditional image segmentation techniques and classification using machine learning techniques still have not achieved the best results. Different image-capturing methods, low-resolution photos, images with a high noise ratio, and other factors contribute to the extraction of low-quality features. This study proposed the Alex net model with absolute rectified linear unit (absRelu) and rectified linear unit (Relu) activation functions. First, the images are read and resized, then passed to convolutional neural networks (CNN) and absRelu or Relu layers to extract the best features. The next step is size reduction using Maxpooling techniques. The output is passed to the dense layers and then to the Softmax classifier. The proposed model was evaluated using three datasets: MMU, AMF, and IITD. Data augmentation was applied to increase the number of samples. For the MMU dataset, the proposed model with absReLu and ReLu yields 0.9866% and 0.9778% in sequence. For the AMF dataset, the proposed model with absRelu and Relu yields 1.0000% and 0.9981% in sequence. With the ITTD dataset, the best results for both absRelu and Relu are 0.9958% and 1.00%, respectively.

Keywords: Eye iris, Pattern recognition, Deep learning, absolute Rectified Linear Unit, Alex net, convolution neural network

تصنيف قزحية العين باستعمال نموذج Alex net مع دالة التفعيل المطلقة

باهرة هاني نايف
قسم علوم الحاسوب,كلية العلوم, جامعة النهرين, بغداد، العراق

الخلاصة:
تمييز وتصنيف قزحية العيون مهمة جدا في تطبيقات تمييز الانماط. لا تزال تقنيات تجزئة الصور التقليدية وتصنيفها باستعمال تقنيات التعلم الآلي لم تحقق أفضل النتائج. بسبب استعمال طرق مختلفة لالتقاط الصور والصور ذات الدقة المنخفضة والصور ذات نسبة التشويش العالية وغيرها من الأسباب التي تؤدي إلى استخراج ميزات منخفضة الجودة. اقترحت هذه الدراسة نموذج Alex net مع دوال التفعيل absolute Rectified Linear Unit (absRelu) و Rectified Linear Unit (Relu) . أولاً، تتم قراءة الصور وتغيير حجمها ثم تمريرها إلى الشبكات العصبية التلافيفية (CNN) وطبقات absRelu أو Relu لاستخراج أفضل الميزات. الخطوة التالية هي تقليل الحجم باستعمال تقنيات Maxpooling. يتم تمرير المخرجات إلى الطبقات الكثيفة

Email: bahera.hani@nahrainuniv.edu.iq

ومن ثم إلى المصنف Softmax. تم تقييم النموذج المقترح باستعمال ثلاث مجموعات بيانات MMU، AMF، وIITD. تم تطبيق زيادة البيانات لزيادة عدد العينات. نتائج النموذج المقترح مع absRelu وRelu هي 0.9866% و0.9778% بالتسلسل لمجموعة بيانات MMU. نتائج النموذج المقترح مع absRelu وRelu هي% 1.0000، و0.9981% بالتسلسل لمجموعة بيانات AMF . باستخدام مجموعة بيانات ITTD، فإن أفضل النتائج لكل من absRelu وRelu هي 0.9958%، و1.0000% على التوالي.

1. INTRODUCTION

Human identification using Iris recognition is the most accurate approach because Iris texture patterns are unique even with identical twins, complex, and stable over time [1, 2]. For these reasons, Iris recognition is a reliable method for a variety of applications such as security control, banking law enforcement, public welfare, and accounting [3]. The performance of Iris recognition depends on extracting features from the segmented images [4]. The traditional methods of iris pattern extraction and recognition can be applied in two steps. The first step involves obtaining handcrafted features through iris segmentation, iris normalization, and feature extraction. These features then advance to the second step for matching, which involves applying machine learning techniques for classification [2, 5]. Some of the traditional methods for extracting patterns are Gabor filter-based Iris code, discrete cosine transform (DCT), discrete Fourier transform (DFT), and Randon transfer [1].

For the past two decades, researchers have turned to deep learning techniques (DL) because they have demonstrated significant success over traditional techniques in various fields of computer vision applications such as face recognition, image captioning, emotion analysis, object detection, feature selection, and classification [6, 7]. DL also proved itself in other fields, such as Natural Language Processing (NLP) tasks such as sentiment analysis, machine translation, name-entity recognition, and question answering [2, 8, 9].

Iris recognition is a very crucial problem, especially in security applications, and requires high-accuracy performance. The traditional techniques of image preprocessing and segmentation consume time and require many algorithms. Such as denoising images, enhancing the image resolution, applying resized images, and then feature extraction. In addition, the image features must be predefined [10, 11]. To overcome all these complications, deep learning techniques are proposed in this study. Although DL techniques require datasets with a large number of samples to obtain high performance, the available Iris datasets are mostly small and not well processed. In addition to using DL, a high-specification GPU processor is required [11].

The paper is structured as follows: Section 2 represents previous research on DL and Iris detection problems. Section 3 presents the proposed methodology. Section 4 presents the results of the experiments. Section 5 presents the comparison with the state of the art.

2. RELATED WORK

This section discusses the latest studies that introduced different methodologies for iris recognition. The authors presented straightforward deep-learning techniques, and some used hybrid methods that included different filters and segmentation techniques in addition to deep-learning techniques for classification.

One of the recent studies related to iris recognition using deep learning is [12]. According to the study, the CASIA, Polaris IITD, Ubiris, and MMU datasets could be used with pre-trained models like Mobile Net, Inception, Nasnet, Efficient Net, VGG 16, and VGG19. The reported results were not sufficient to show the performance of the proposed models.

F. Jan et al. [13] proposed a robust iris localization system. The study's goal is to maintain localization speed and accuracy. The study suggested a set of methods, such as preprocessing the eye image with an order statistic filter and bilinear interpolation, getting adaptive thresholds from image histograms, using morphological operators to process binary images, using the geometry concept to get the center of the pupil, and using the circular hough transformation to mark the edge of the iris. Three datasets were used: the CASIA-Iris3-Interval, IITD V1.0, and MMU V1.0. The results of the proposed method outperformed the state-of-the-art studies. Nevertheless, the proposed system contains too many techniques and is time-consuming. The obtained accuracy rates for CASIA-Iris3-Interval, IITD V1.0, and MMU V1.0 are 99.3%, 99.5%, and 99.34%, respectively.

J. Jayanthi et al. [6] introduced another study to detect and recognize the human iris. The authors used the same image preprocessing and segmentation techniques in the study of F. Jan et. al. [13], but they applied Mask R-CNN for iris recognition. The authors claimed that the proposed method showed better performance than VGG16, Alex Net, and other deep-learning models. Similar to F. Jan et al. [13], they solved the problem by extracting the correct threshold and detecting the correct pupil center and radius. Additionally, the results depend on the correct pupil boundary detection. However, the proposed model outperformed the Alex Net and VGG16 models with a maximum recognition accuracy of 99.14%.

H. M. Therar et al. [14] proposed another study for iris recognition (left and right) using convolutional neural networks and transfer learning techniques. The authors evaluated the proposed method using the IITD and CASIA-Iris-V3 datasets. The authors declared that the proposed method showed outstanding results in comparison to state-of-the-art studies. The proposed model had an accuracy of 99% for both the left and right IITD iris datasets and 94% and 93% for the left and right iris for the CASIA-iris-V3 interval datasets, respectively.
According to S. Barra et al. [15], iris segmentation should be done in three steps: ROI detection using the Hough transform; iris clustering using simple linear iterative and SKEG (Skewness, Kurtosis, Entropy, and Gini index) estimation; and evaluation of fuzzy rules and noisy clusters using fuzzy controllers. The best recognition rate for the MICHE dataset was 76.67%.

Y. Chen et. al. [16] presented a simple deep-learning model for iris segmentation. The proposed model has two parts. The first part, known as the dense encoder, comprises two CNN layers, a normalization layer, and two pooling layers. The second part, known as the dense decoder, involves upsampling the pixels to construct the image. The authors evaluated the proposed model using three iris datasets: CASIA-Interval-V4, IITD, and UBIRIS-V2. The authors claimed that the proposed model outperforms state-of-the-art studies. A small number of images, however, are misclassified as iris due to non-ideal labeling conditions. The same methodology proposed by [17, 18] was discussed using FRED-Net (a fully residual encoder-decoder network) for accurate iris segmentation captured by different devices. The proposed model gets 99.05% of the iris dataset CASIA-Interval-V4, 98.84% of the IITD dataset, and 99.47% of the UBIRIS.V2 dataset right.

Moreover, M. Liu et al. [19] discussed iris segmentation using segmentation techniques such as Gaussian, triangular fuzzy average, and triangular fuzzy median smoothing filters. After filtering the image pixels, the study used a CNN pipeline to extract pixel features and find matching labels. The study tested the proposed model using CASIA-IrisV4, Vista, and ATVS-FIr datasets, and the accuracy rates are 83.1%, 88.4%, and 89.2 in turn. The resulting accuracy rates were not better than the state-of-the-art. Using a set of filters may have resulted in information loss.

M. B. Lee et al. [20] propose data augmentation to address the scarcity of samples in the iris dataset. The study proposed the augmentation-based conditional generative adversarial network (cGAN) model. According to the authors, the proposed method showed better results using three datasets: the NICE, MICHE, and CASIA-Iris-distance datasets. The resulting error rates are 12.79%, 8.58%, and 2.69%, respectively.

In summary, deep learning techniques showed remarkable results. All the studies that have been presented have solely focused on applying well-known deep learning models without any consideration for enhancing and modifying the deep learning functions, such as the activation or loss functions. This encourages us to search in this direction and propose an absolute rectified linear unit (absRelu).

3. PROPOSED METHODOLOGY

For the past two decades, many different deep-learning models have been introduced by the researchers, such as LeNet-5 [21], the Alex Net network was introduced in 2012 in the Image Large Scale Visual Competition (ILSVRC) [22], VGG12 Net, VGG13, 16, 19 [23], and the ZFNet architecture was proposed by M. D. Zeiler and R. Fergus [24]. This paper applies the modified Alex Net architecture to a small dataset.

3.1 Alex net structure

In 2012, the Image Large Scale Visual Competition (ILSVRC) introduced the AlexNet network, which ranked first in the techniques competition. Alex Net, as shown in Figure. 1, consists of eight layers in total. Five layers are the convolution layers with the Relu activation function, and the rest are the fully connected layers. The SoftMax layer receives the final FC layer's output, which contains 1000 possible prediction labels with 0–1 probabilities [22]. Alex Net's major development involved enhancing performance by deepening learning and incorporating regularization into CNN networks to prevent overfitting issues.

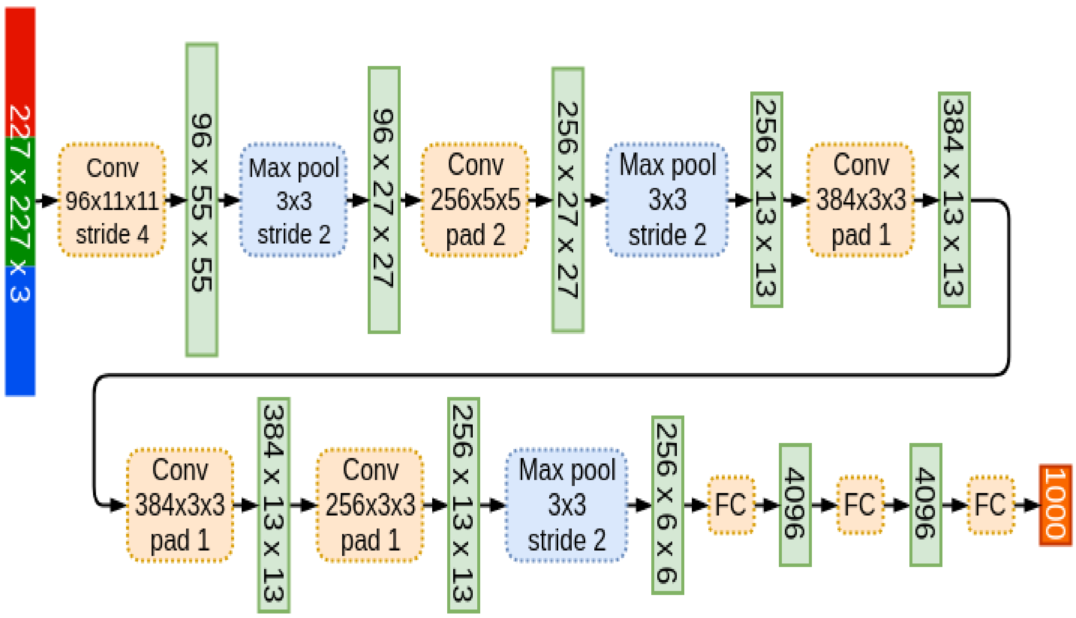

Figure 1: Alex net architecture Source: [22]

3.2 Convolution Neural Networks

A convolutional neural network (CNN) is an artificial neural network that has become extremely popular in deep pattern recognition learning fields. Deep CNN is the first fully supervised-trained model using state-of-the-art approaches [25]. The majority of researchers were drawn to CNN due to its exceptional accuracy in training vast amounts of data [26], its low error rate, and its rapid performance in digit classification across multiple categories or classes with dropout [27]. On the other hand, it needs a very high-speed processing unit, huge storage, and large-scale recognition [28].

The most powerful deep neural network is the convolutional neural network (CNN) [26]. The three main things that the convolutional neural network (CNN) does are convolution filtering, pooling, and the activation function, which is mainly nonlinear or acts as a nonlinear function [22, 29].

For an input image of two dimensions and a kernel (kr) of dimension M×N. In the convolution phase, the feature map is plotted by skimming the kernel over the input values. The feature map was extracted using Eq. 1.

$$C_r(i,j) = \sum_{m=1}^{M}\sum_{n=1}^{N} I\,(i+m, j+n)\; k_r\,(m,n), \tag{1}$$

The feature map size became an array of three dimensions (I×J×R), where R represents the number of kernels used in the convolution phase. The following Example explains the convolution process:

Suppose an input image block of size (8×8) and the kernel size is (3×3) as in Figure 2:

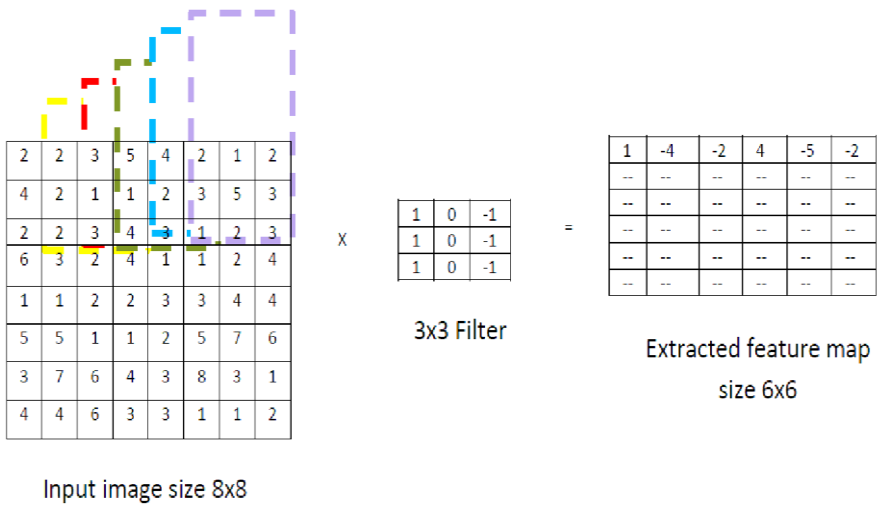

Figure 2: A convolution filter of size 3 x 3 to an input image of size 8x8 to produce a feature map of size 8x8

Each value from the kernel will be multiplied by each pixel in the (3×3) window from the input image. Then sum the result of each multiplication step. The result will replace the value of the center pixel in the window (3×3).

The(3×3) window will be shifted to the right by one column (1 stride) and the multiplication process to find the next convoluted feature until no more windows can be applied. The next step is moving down one row and repeating the previous steps until no more rows are convoluted.

3.3 *Max Pooling*

The main goal of using the pooling technique is to reduce the size of the output extracted feature maps to suit the network's output layer size, which represents the number of dataset classes [30]. The advantages of the pooling layer are dimensionality reduction, reduced processing complexity, and speeding up the training process. The pooling function is shown in Eq. 2 [30].

$$S_r(i,j) = \left[\sum_{h=-k/2}^{k/2} \sum_{w=-k/2}^{k/2} \left|f_{g(h,w,i,j,r)}\right|^p\right]^{\frac{1}{p}}, \quad (2)$$

where k = pooling size, d= feature map progress, $g(h,w,i,j,r)_{=}(d.i+h,r.j+w,r)$, p= norm subsampling, and when p=∞ , it is Maxpooling [30]. Figure.3 explains an example of the Maxpooling process.

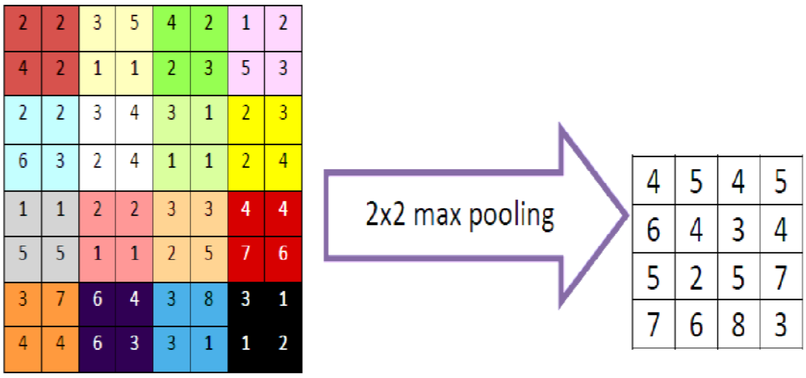

Figure 3: The max-pooling process with size 2 × 2

3.4 *The Rectified Linear Unit (ReLU)*

A nonlinear activation function is applied for each feature in the feature map. The rectified linear unit is one of the most popular in DNN because it is easy to optimize due to linear similarity to linear units [31]. The output of the ReLU operation is 0 for the most second derivatives and equal to 1 when the Relu operation is active [32]. The rectified linear unit (ReLu) function considers all the input values $x < 0$ are equal to 0. So, the gradient is positive, as shown in Figure. 4 This is considered a limitation for Relu when there are negative samples. The function formula is as in Eq. 3 [33].

$$z_j = f(x_j) = Max\ (0, x_j), \quad (3)$$

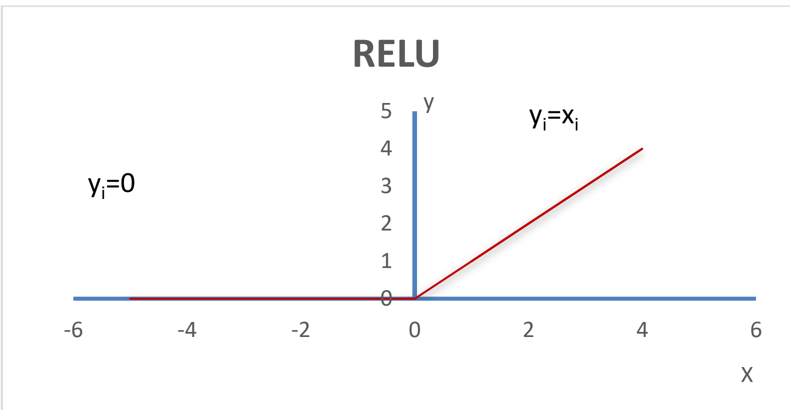

Figure 4: The performance of Relu with input $x \geq 0$ and $x < 0$

3.5 The proposed Absolute Relu

In deep learning, Relu activates the neural units of the input feature maps with values greater than zero $(x \geq 0)$ and the output is a linear function of z. All the other units with input values less than 0 ($x < 0$) will be set to OFF for the next training process. This leads to minimizing the size of the trained network and the trained samples [34].

Various studies are proposed to overcome the limitation of Relu [35]. In this paper, an absolute Relu is proposed to activate negative input features of the hidden layers by applying the absolute function to the input negative features to be activated as the positive samples. In this way, the total number of samples will be activated and passed to the next layer. The function can be represented as follows in Eq. 4:

$$f(x_{ij}) = \begin{bmatrix} x & if & x_{ij} \geq 0 \\ |x| & if & x_{ij} < 0 \end{bmatrix}, \quad (4)$$

Where:

x is the input feature, i *and* j are the input feature index.

the absRelu function will be as follows in Eq.5 and Figure.5:

$$f(x_{ij}) = Max\,(x_{ij}, 0) + \,min\,(|x_{ij}|, 0) \quad (5)$$

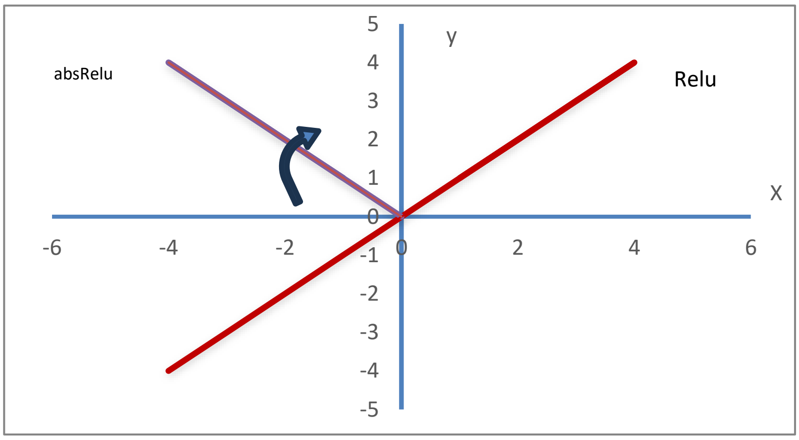

Figure 5: The green arrow represents the proposed absRelu when $x < 0$. The blue line represenst Relu when $x \geq 0$

3.6 The proposed Alex net CNN model

The model consists of a set of five convolutional neural networks (CNN). The structure of the proposed model is shown in Figure. 6. Each CNN layer is followed by a Maxpooling layer. To obtain high performance from the model, a small alteration in the number of extracted features is applied. The extracted features from the CNN layer are as follows: 20, 50, 60, 60, and 60 using the rectified linear unit (Relu) and the proposed absolute rectified linear unit (absRelu). The kernel sizes are (11,11), (5,5), (3,3), (3,3), and (3,3). Two dense layers of five hundred units and one dense layer for the classifier with the number of labels. In addition, there are two dropout layers of 0.1 and 0.5 between the dense layers. The input image is of size (100×100). Before passing the images to the AlexNet model, an augmentation technique is applied to increase the number of samples.

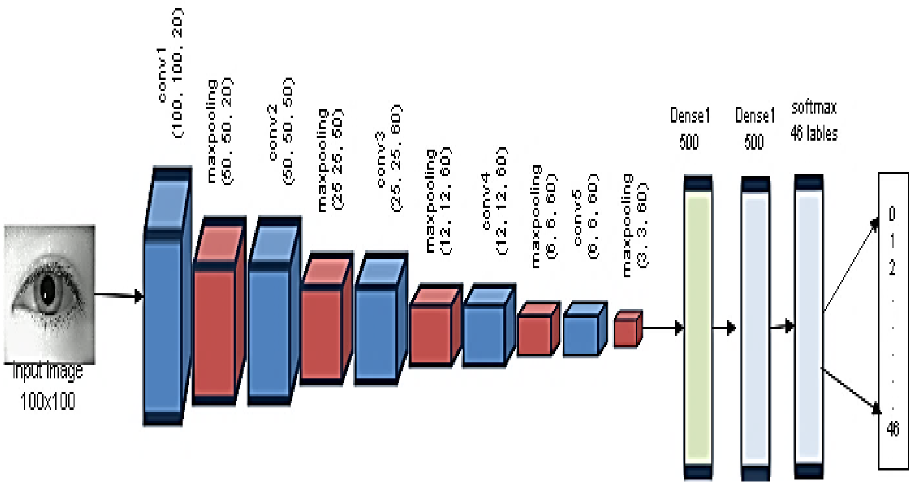

Figure 6: The proposed block diagram of Alex net model structure with MMU dataset with 46 class labels.

3.7 The datasets

Figure. 7 presents the evaluation of the proposed model using three iris datasets. The first one is the MMU1 database, which was collected for the iris biometric attendance system at Multimedia University. It consists of five bitmap images of forty-six people, each on the left and right, for a total of 460 images. The size of each is 320x240. The master's degree student created the second dataset, Ahmed Myasar Fathi (AMF), from the University of Mosul. It consists of 540 samples of iris images in bitmap format collected from fifty-four participants at a rate of ten images per participant with size 640 x 480. Five images for the left eye and five for the right eye. The ages of the participants ranged between 20 and 50 years old. Data augmentation for both datasets is applied to increase the number of samples to 2650. Therefore, each image undergoes rotation at four different angles (5, 10, -5, -10). The third dataset, IITD, consists of the iris images collected from the students and staff at IIT Delhi, India. From January to July 2007, the Biometrics Research Laboratory acquired this database using a JIRIS, JPC1000 digital CMOS camera. The acquired images were saved in bitmap format. The database of 2240 images was acquired from 224 different users and made available freely to the researchers. All the subjects in the database are in the age group of 14–55 years, comprising 176 males and 48 females. These images have a resolution of 320 x 240 pixels, and all of them were taken in an indoor environment. All the images in the database were acquired from volunteers who were not paid or provided any honorarium. The images were acquired using an automated program that requires users to present their eyes in a sequence until ten images are registered. All the samples in the three datasets are resized to 100x100.

MMU dataset samples			
	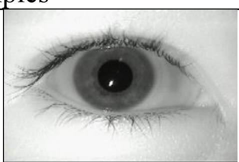	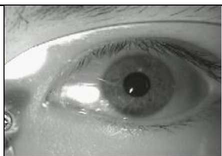	
aeva-L	Aeva-R	chongpkl-L	Chongpkl-R
AMF dataset samples			

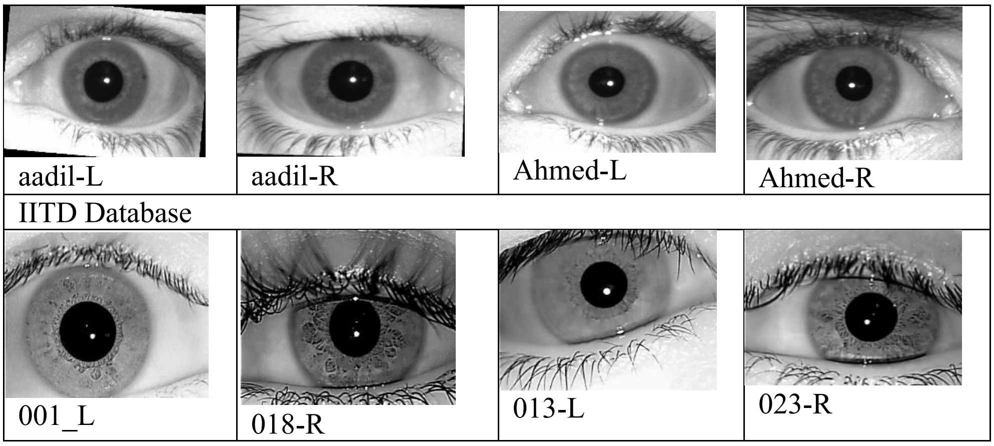

Figure 7: Samples from the used datasets (L-Left, R-Right)

4. Experiments and Results

To evaluate the performance of the proposed model, two experiments were conducted to determine if the proposed model is significant or not for both datasets.

4.1 Experiment 1: The proposed Absolute Relu and Relu with MMU dataset.

In this experiment, the study evaluated the performance of the proposed absolute Relu and the standard Relu with the MMU dataset. The dataset is split into 60% for training, 20% for validation, and 20% for testing. The proposed model was trained for 70 epochs using absRelu and Relu separately. Table 1 and Figureure 8 display the results.

Table 1: The performance of the proposed absRelu and Relu with MMU

Model	Training accuracy	Loss rate	Validation accuracy	Loss Rate	Testing accuracy	Loss rate
Relu	0.9826	0.0355	0.9833	0.0236	0.9778	0.0532
absRelu	0.9729	0.0932	0.9889	0.0778	0.9866	0.0372

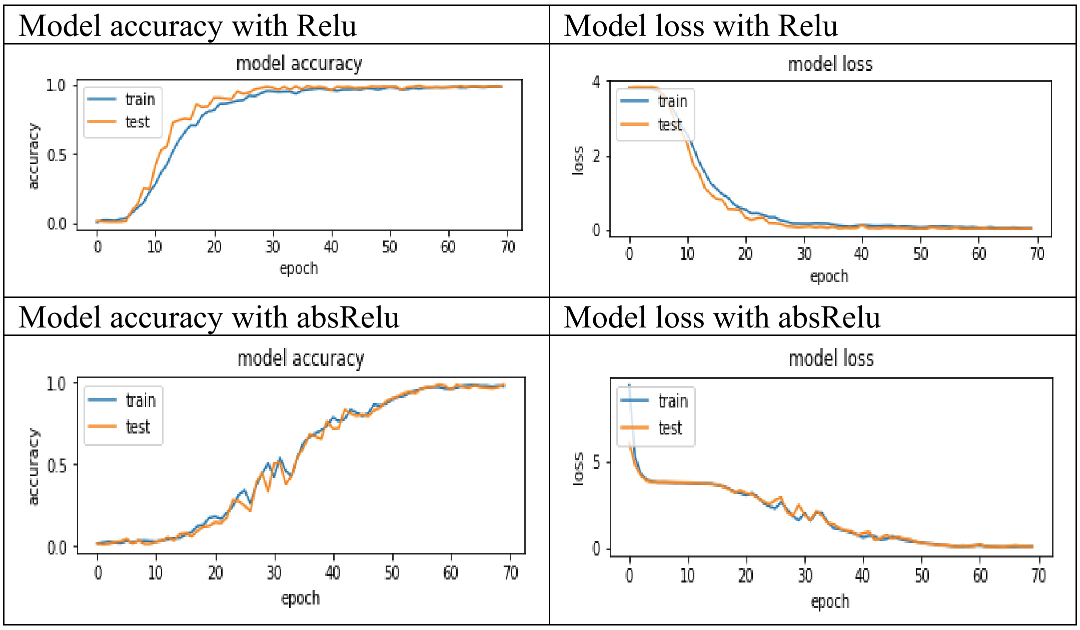

Figure 8: The performance of Relu and AbsRelu with MMU dataset for 70 epochs.

The results indicated that the proposed absRelu performed slightly better than the Relu activation function. However, the Relu activation function showed a smooth increase in the training and evaluation accuracy rate, as shown in Figure. 8. Unlike the proposed absRelu, which displayed unstable performance for 60 epochs before stabilizing, the Relu activation function showed a smooth increase in the training and evaluation accuracy rate, as shown in Figure. 8. This can be attributed to the fact that the epoch in question contained samples with ineffective features. These features with Relu are represented by zero and will never be activated in the future. Figureures 9 and 10 display examples of the extracted features from the intermediate CNN layers for both activation functions (Relu and absRelu).

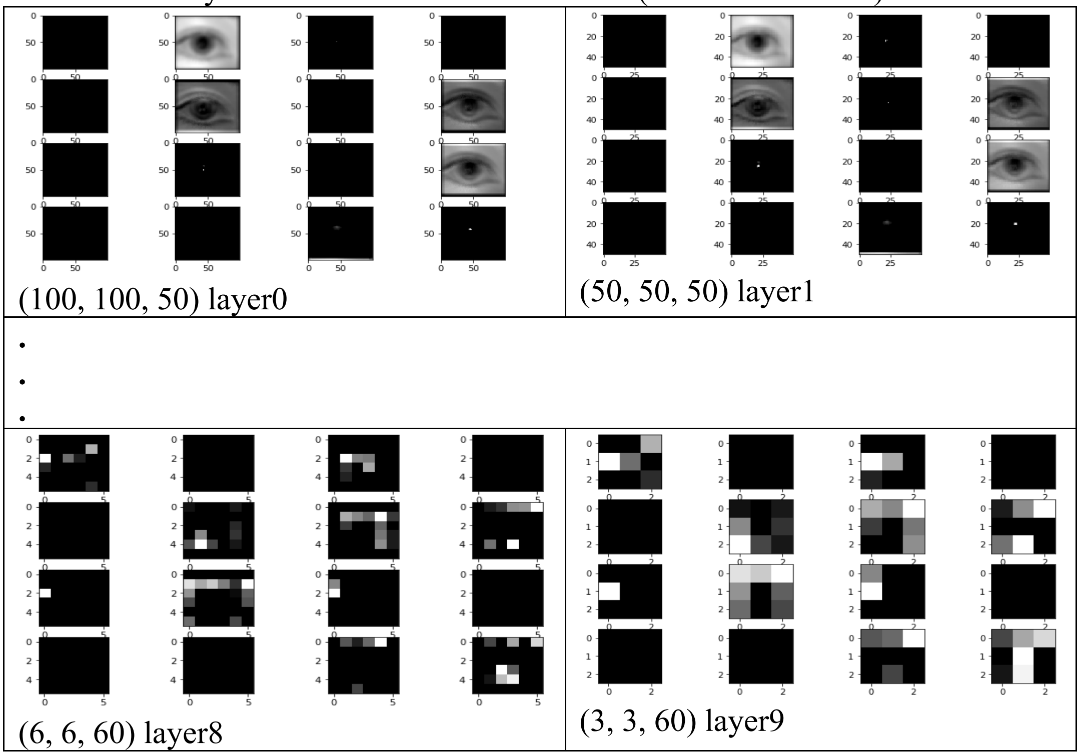

Figure 9: Samples from intermediate CNN layers and the activated Features for MMU dataset and Relu

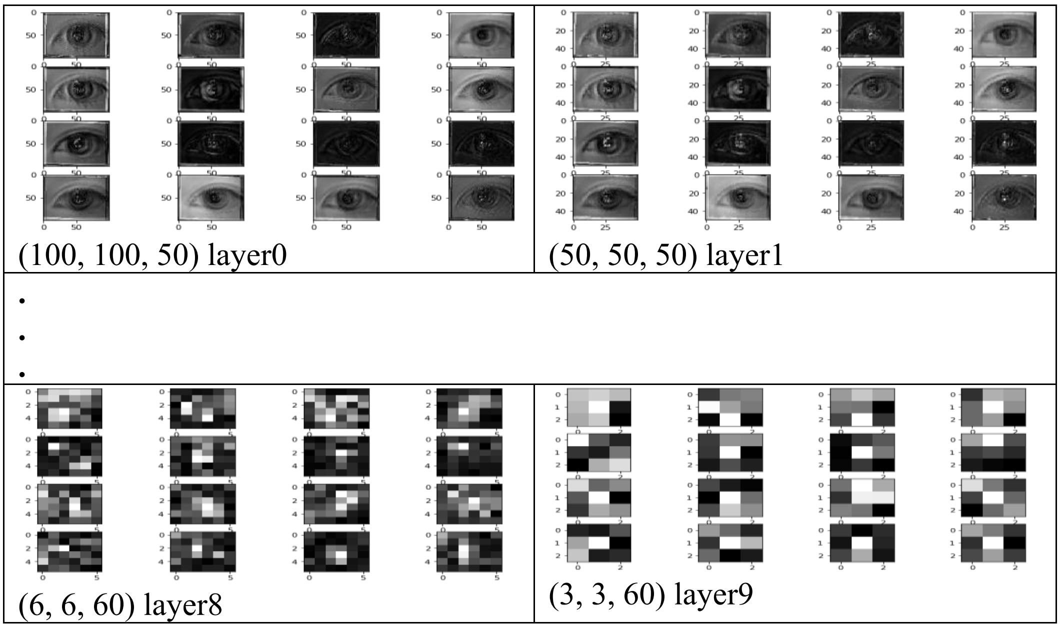

Figure 10: Samples from intermediate CNN layers and the activated Features for MMU dataset and absRelu.

4.2 Experiment 2: The proposed Absolute Relu and Relu with AMF dataset.

Another iris dataset called AMF is used to classify fifty-four participants according to their eye iris. Also, AbsRelu and Relu are used to activate the image features using a set of CNN and max-pooling layers as described in the Alex net model. The dense layers receive the activated features before the classifier, SoftMax, classifies the images. The results are presented in Table 2 and Figure. 11.

Table 2: The performance of the proposed absRelu and Relu with AMF

Model	Training accuracy	Loss rate	Validation accuracy	Loss Rate	Testing accuracy	Losee rate
Relu	0.9988	0.0039	0.9976	0.0033	0.9981	0.0122
absRelu	0.9823	0.0531	1.0000	5.3361e-04	1.0000	6.3960e-04

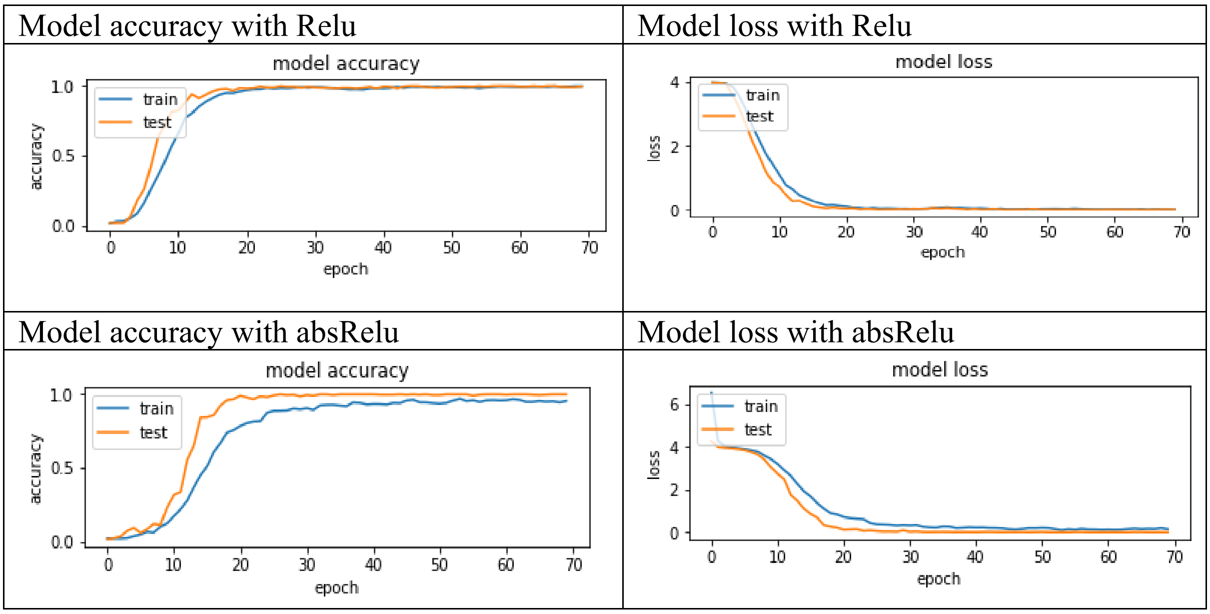

Figure 11: The performance of Relu and AbsRelu with the AMF dataset for 70 epochs

Figureures 12 and 13 present all the intermediate CNN layers for the MFA dataset, including Relu and absRelu values. Each layer shows the extracted features from CNN. The classifier will use the layer's features to classify the image.

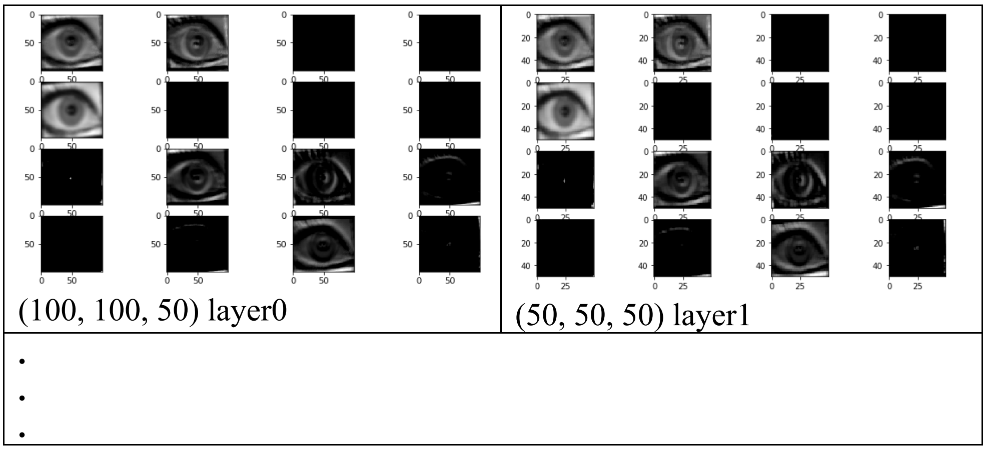

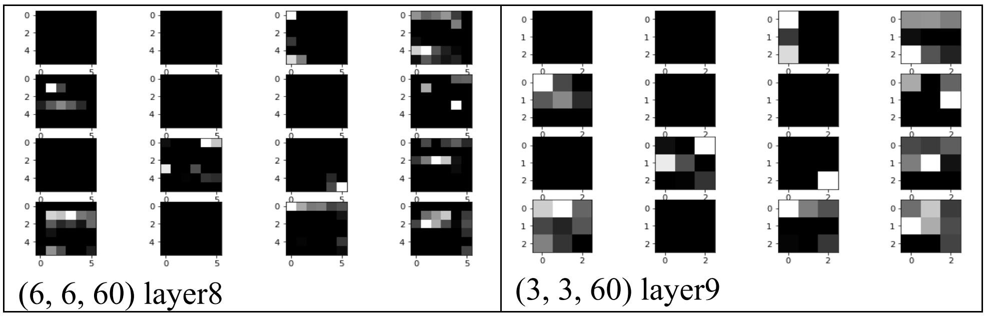

Figure 12: Samples from intermediate CNN layers and the activated Features for the AMF dataset and Relu

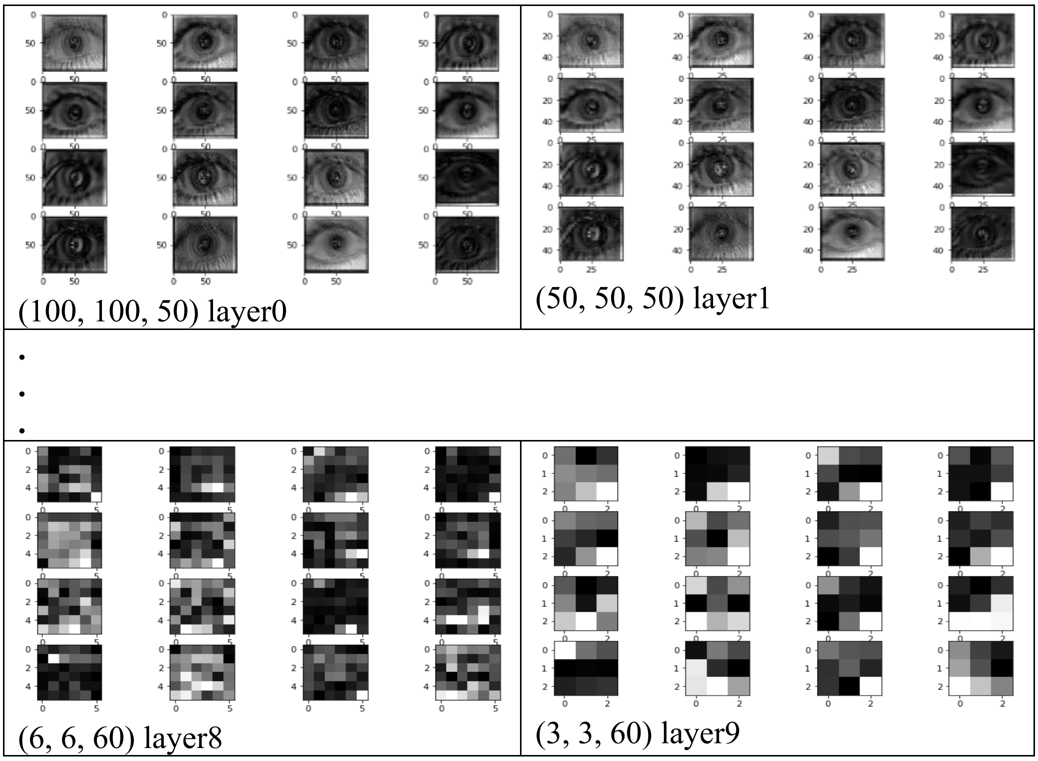

Figure 13: Samples from intermediate CNN layers and the activated Features for the AMF dataset and absRelu

Figure (9–13) clearly demonstrate that absRelu activates all the extracted features. Conversely, Relu does not activate the feature with values less than 0, setting it equal to zero and deactivating the neural unit for the remainder of the training process. Each CNN layer presents these inactivated features in black.

4.3 Experiment 3: The proposed Absolute Relu and Relu with the IITD database

The IITD database contains the iris images of 224 participants, who are students and staff members at IIT Delhi, India. The dataset was collected between January and July 2007 using a JIRIS, JPC1000 digital CMOS camera. The database included a set of left (L) and right (R) iris images for 211 participants. For the rest of the thirteen participants, only left-iris images were collected. The experiment was conducted using the Alex net model with Relu and absRelu activation functions for 70 epochs. The results are presented in Table 3 and Figures. 14, 15, and 16.

Table 3: Presents the results of the IITD database with Relu and absRelu using the Alex net model

Model	Training accuracy	Loss rate	Validation accuracy	Loss Rate	Testing accuracy	Loss rate
Relu	0.9966	0.0109	0.9968	0.0080	1.0000	0.0024
absRelu	0.9848	0.0492	0.9974	0.0128	0.9958	0.0189

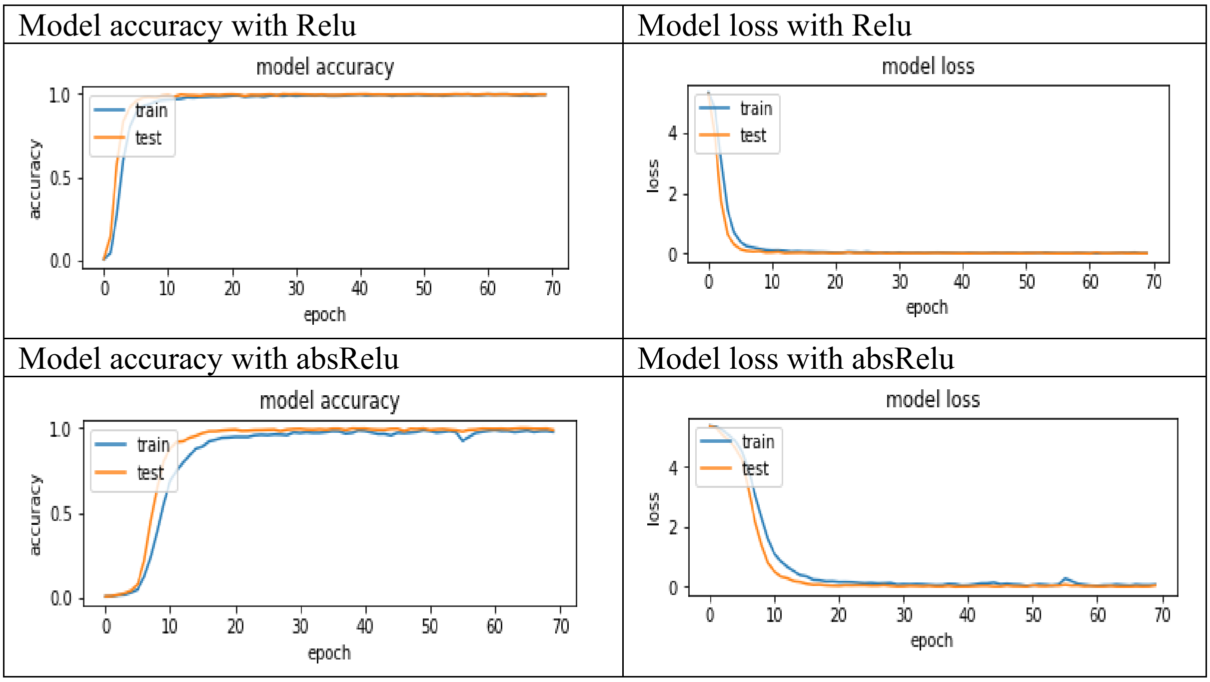

Figure 14: The accuracy and loss rates of training the ITTD dataset with the Alex net model using Relu and absRelu activation functions

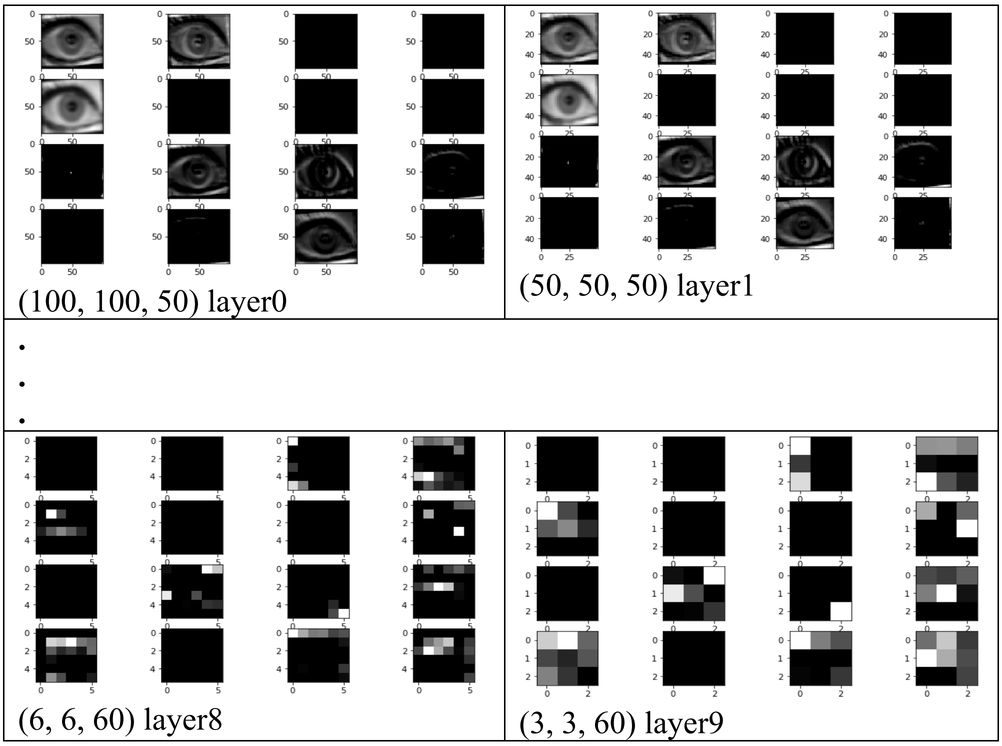

Figure 15: Samples from intermediate CNN layers and the activated Features for the ITTD dataset and Relu

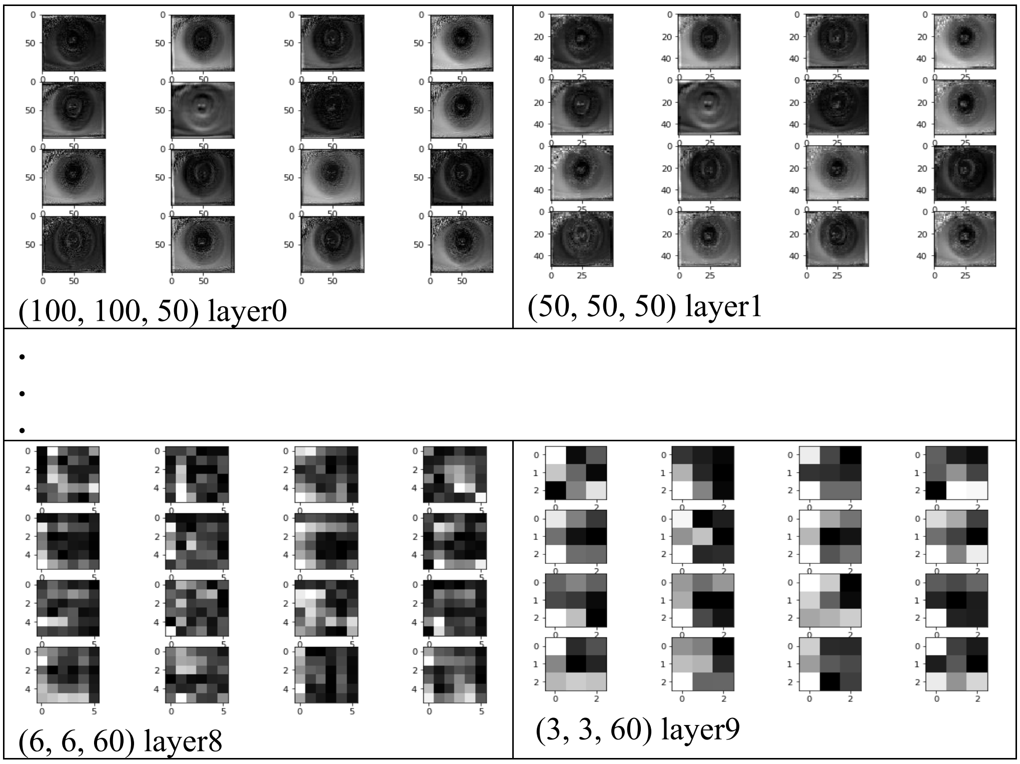

Figure 16: Samples from intermediate CNN layers and the activated Features for the ITTD dataset and absRelu

4.4 Samples from the predicted classes

More results are presented in this section related to the predicted labels from MMU, AMF, and IIDT datasets with the proposed absRelu as shown in Figure. 17. As clear, all the predicted classes are correct and match the true class

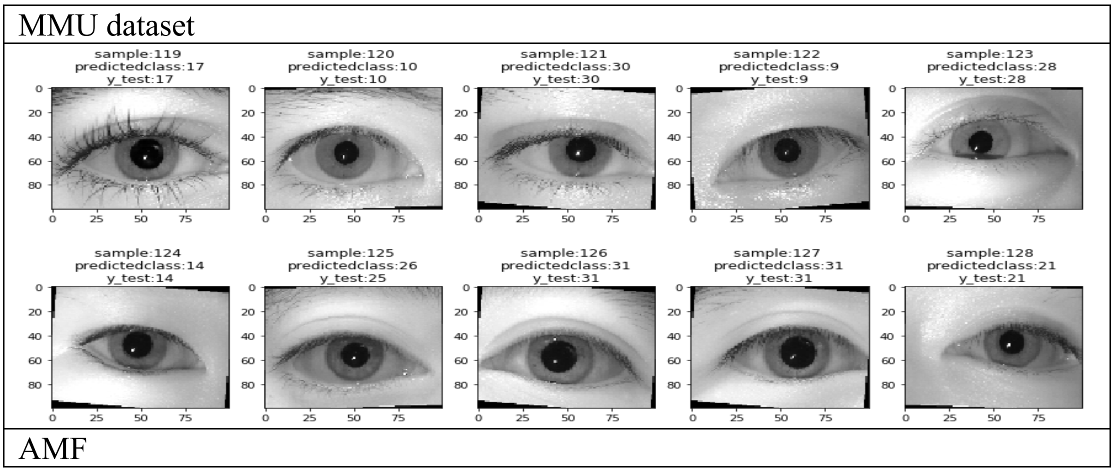

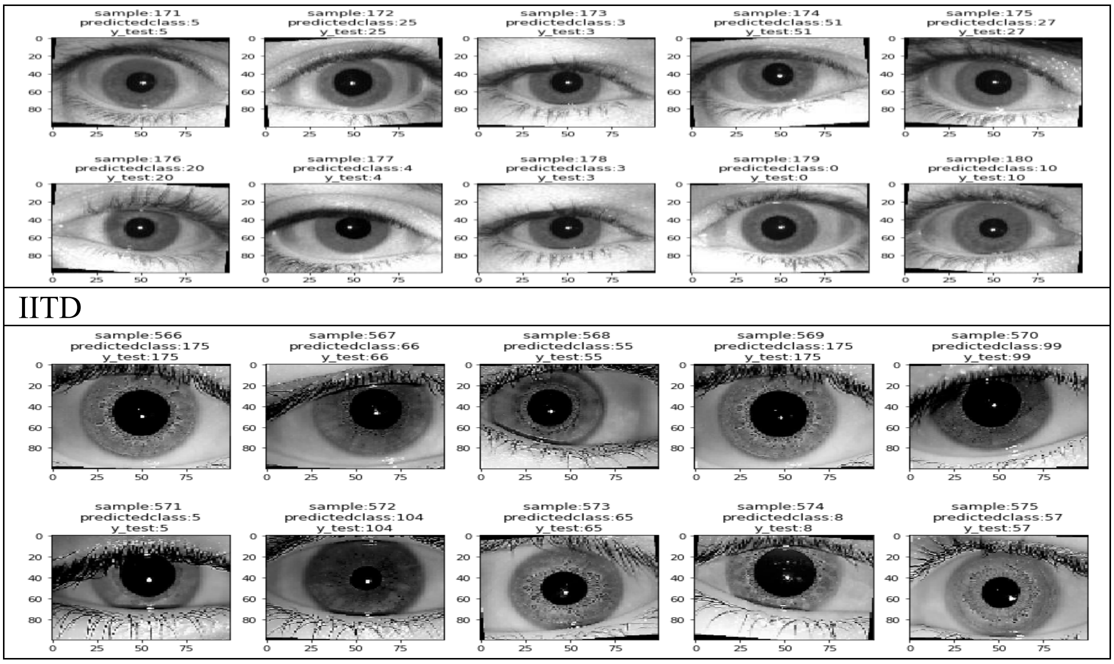

Figure 17: Samples from the predicted labels for MMU and AMF dataset

5. Comparison With the State-Of-Art

Table 4 presents the latest state-of-the-art study results. As shown in the table, the proposed methodology outperforms state-of-the-art studies.

Table 4: Comparison between the proposed absRelu and the state-of-are studies.

The study	Datasets	Accuracy Rates
[19]	CASIA, Cogent, Vista, ATVS	72.9-82.8%
[15]	MICHE	71.67%
[16]	CASIA interval, ITTD, UBIRIS	99.5%, 98%, 99.45
[14]	ITTD left, ITTD right	96%, 96.26%
[36]	CASIA Iris Image	94% best
Proposed absRelu	**MMU, AMF, IITD**	**98.66%, 100%, 100%**

Discussion

The study discussed the classification and recognition of the human iris. The eye-iris classification is one of the biometric techniques used in security systems. The study proposed an absRelu activation function, which activates the extracted positive and negative features using a set of CNN layers known as the Alex net model. The results are compared with the Relu activation function. To evaluate the proposed model, three datasets were used: the MMU, AMF, and ITTD. Also, the results are presented in the form of an accuracy rate and a loss rate. In addition, samples from the intermediate performance of CNN were presented to show the steps of extracting features with Relu and absRelu. A sample from the predicted classes is also presented to show the accuracy of the prediction from the test dataset. All of the results showed that the proposed method's performance is significant and surpasses that of state-of-the-art studies. More experiments were conducted with different datasets to prove the functionality of absRelu, such as the digit MNIST and Arabic characters datasets introduced by [10]. The proposed model's performance showed meaningful results of 0.9932% with MINIST and 0.9436 for Arabic handwritten characters.

Since the dataset size is limited, future work will focus on how to increase the available sample number by applying sample generation techniques such as the generative adversarial network (GAN).

Funding
None
Acknowledgment
My heartfelt thanks to the students and staff members at IIT Delhi, India, for their contribution to the IITD dataset.

Conflicts Of Interest

The author declares no conflict of interest. In addition, I confirm that all the Figures and tables in the manuscript belong to the author's work except Figure. 1, and the citation is added.

References

[1] K. Yang, Z. Xu, and J. Fei, "Dualsanet: Dual spatial attention network for iris recognition," in *Proceedings of the IEEE/CVF Winter Conference on Applications of Computer Vision*, pp. 889-897,2021.
[2] S. Minaee and A. Abdolrashidi, "Deepiris: Iris recognition using a deep learning approach," *arXiv preprint arXiv:1907.09380,* 2019.
[3] J. Daugman, "Iris recognition border-crossing system in the UAE," *International Airport Review,* vol. 8, no. 2, 2004.
[4] K. W. Bowyer, K. Hollingsworth, and P. J. Flynn, "Image understanding for iris biometrics: A survey," *Computer vision and image understanding,* vol. 110, no. 2, pp. 281-307, 2008.
[5] F. He, Y. Han, H. Wang, J. Ji, Y. Liu, and Z. Ma, "Deep learning architecture for iris recognition based on optimal Gabor filters and deep belief network," *Journal of Electronic Imaging,* vol. 26, no. 2, pp. 023005-023005, 2017.
[6] J. Jayanthi, E. L. Lydia, N. Krishnaraj, T. Jayasankar, R. L. Babu, and R. A. Suji, "An effective deep learning features based integrated framework for iris detection and recognition," *Journal of ambient intelligence and humanized computing,* vol. 12, pp. 3271-3281, 2021.
[7] H. A. Naman and Z. J. M. Ameen, "A New Method in Feature Selection based on Deep Reinforcement Learning in Domain Adaptation," *Iraqi Journal of Science,* pp. 817-829, 2022.
[8] A. A.-R. Hussien and N. A. Abdullah, "A Review for Arabic Sentiment Analysis Using Deep Learning," *Iraqi Journal of Science,* vol. 64, no. 12, pp. 6572–6585, Dec. 2023, doi: 10.24996/ijs.2023.64.12.37.
[9] M. A. H. Wadud, M. Mridha, and M. M. Rahman, "Word embedding methods for word representation in deep learning for natural language processing," *Iraqi Journal of Science,* vol. 63, no. 3, pp. 1349–1361, Mar. 2022, doi: 10.24996/ijs.2022.63.3.37.
[10] B. H. Nayef, S. N. H. S. Abdullah, R. Sulaiman, and Z. A. A. Alyasseri, "Optimized leaky ReLU for handwritten Arabic character recognition using convolution neural networks," *Multimedia Tools and Applications,* pp. 1-30, 2022.
[11] S. C. Yow and A. N. Ali, "Iris recognition system (IRS) using deep learning technique," *Journal of Engineering Science,* vol. 15, no. 2, pp. 125-144, 2019.
[12] M. H. MK and M. S. Kumari, "PERFORMANCE ANALYSIS OF DEEP LEARNING MODELS FOR IRIS RECOGNITION," *Semiconductor Optoelectronics,* vol. 42, no. 1, pp. 113-123, 2023.
[13] F. Jan, N. Min-Allah, S. Agha, I. Usman, and I. Khan, "A robust iris localization scheme for the iris recognition," *Multimedia Tools and Applications,* vol. 80, pp. 4579-4605, 2021.
[14] H. M. Therar, L. D. E. A. Mohammed, and A. J. Ali, "Multibiometric system for iris recognition based convolutional neural network and transfer learning," in *IOP Conference Series: Materials Science and Engineering*, 2021, vol. 1105, no. 1: IOP Publishing, p. 012032.
[15] S. Barra, C. Bisogni, M. Nappi, and S. Ricciardi, "F-FID: fast fuzzy-based iris de-noising for mobile security applications," *Multimedia Tools and Applications,* vol. 78, pp. 14045-14065, 2019.

[16] Y. Chen, W. Wang, Z. Zeng, and Y. Wang, "An adaptive CNNs technology for robust iris segmentation," *IEEE Access,* vol. 7, pp. 64517-64532, 2019.
[17] M. Arsalan, D. S. Kim, M. B. Lee, M. Owais, and K. R. Park, "FRED-Net: Fully residual encoder–decoder network for accurate iris segmentation," *Expert Systems with Applications,* vol. 122, pp. 217-241, 2019.
[18] K. Wang and A. Kumar, "Toward more accurate iris recognition using dilated residual features," *IEEE Transactions on Information Forensics and Security,* vol. 14, no. 12, pp. 3233-3245, 2019.
[19] M. Liu, Z. Zhou, P. Shang, and D. Xu, "Fuzzified image enhancement for deep learning in iris recognition," *IEEE Transactions on Fuzzy Systems,* vol. 28, no. 1, pp. 92-99, 2019.
[20] M. B. Lee, Y. H. Kim, and K. R. Park, "Conditional generative adversarial network-based data augmentation for enhancement of iris recognition accuracy," *IEEE Access,* vol. 7, pp. 122134-122152, 2019.
[21] Y. LeCun *et al.*, "Backpropagation applied to handwritten zip code recognition," *Neural computation,* vol. 1, no. 4, pp. 541-551, 1989.
[22] A. Krizhevsky, I. Sutskever, and G. E. Hinton, "Imagenet classification with deep convolutional neural networks," in *Advances in neural information processing systems*, 2012, pp. 1097-1105.
[23] K. He, Y. Wang, and J. Hopcroft, *A Powerful Generative Model Using Random Weights for the Deep Image Representation*. 2016.
[24] M. D. Zeiler and R. Fergus, "Visualizing and understanding convolutional networks," in *European conference on computer vision*, 2014: Springer, pp. 818-833.
[25] J. Donahue *et al.*, "Decaf: A deep convolutional activation feature for generic visual recognition," in *International conference on machine learning*, 2014, pp. 647-655.
[26] Y. LeCun and Y. Bengio, "Convolutional networks for images, speech, and time series," *The handbook of brain theory and neural networks,* vol. 3361, no. 10, p. 1995, 1995.
[27] J. Deng, W. Dong, R. Socher, L.-J. Li, K. Li, and L. Fei-Fei, "Imagenet: A large-scale hierarchical image database," in *2009 IEEE conference on computer vision and pattern recognition*, 2009: IEEE, pp. 248-255.
[28] O. Russakovsky *et al.*, "Imagenet large scale visual recognition challenge," *International journal of computer vision,* vol. 115, no. 3, pp. 211-252, 2015.
[29] J. Schmidhuber, "Deep learning in neural networks: An overview," *Neural Networks,* vol. 61, pp. 85-117, 2015/01/01/ 2015.
[30] B. Chen, W. Deng, and J. Du, *Noisy Softmax: Improving the Generalization Ability of DCNN via Postponing the Early Softmax Saturation*. 2017.
[31] R. H. Hahnloser, R. Sarpeshkar, M. A. Mahowald, R. J. Douglas, and H. S. Seung, "Digital selection and analogue amplification coexist in a cortex-inspired silicon circuit," *Nature,* vol. 405, no. 6789, p. 947, 2000.
[32] I. Goodfellow, Y. Bengio, and A. Courville, *Deep learning*. MIT press, 2016.
[33] K. Jarrett, K. Kavukcuoglu, M. Ranzato, and Y. LeCun, "What is the best multi-stage architecture for object recognition? In (ICCV'09)," *IEEE,* vol. 4, no. 6, p. 7, 2009.
[34] B. H. Nayef, S. N. H. Sheikh Abdullah, R. Sulaiman, and Z. A. A. K. Alyasseri, "VARIANTS OF NEURAL NETWORKS: A REVIEW," *Malaysian Journal of Computer Science,* vol. 35, no. 2, pp. 158-178, 04/29 2022. [Online]. Available: https://ejournal.um.edu.my /index.php/MJCS /article/view/28792.
[35] B. H. Nayef, S. N. H. S. Abdullah, R. Sulaiman, and Z. A. A. Alyasseri, "Optimized leaky ReLU for handwritten Arabic character recognition using convolution neural networks," *Multimedia Tools and Applications,* 2021/10/19 2021, doi: 10.1007/s11042-021-11593-6.
[36] Y. Wei, X. Zhang, A. Zeng, and H. Huang, "Iris Recognition Method Based on Parallel Iris Localization Algorithm and Deep Learning Iris Verification," *Sensors,* vol. 22, no. 20, p. 7723, 2022.